Journal of Marine Science and Technology

Volume 25 | Issue 6 Article 20

CYCLIC SHEAR BEHAVIOR CHARACTERISTICS OF MARINE SILTY SAND

Su Won Son
Department of Civil and Environment Engineering, Pusan National University, Busan, Korea.

Min Jae Ko
Department of Civil and Environment Engineering, Pusan National University, Busan, Korea.

Jin Man Kim
Department of Civil and Environment Engineering, Pusan National University, Busan, Korea., jmkim@pusan.ac.kr

CYCLIC SHEAR BEHAVIOR CHARACTERISTICS OF MARINE SILTY SAND

Acknowledgements

This research was supported by the Basic Science Research Program funded by the National Research Foundation of Korea. We are grateful for their support. (NRF-2017R1A2B4010201)

Journal of Marine Science and Technology, Vol. 25, No. 6, pp. 784-790 (2017)
DOI: 10.6119/JMST-017-1226-20

CYCLIC SHEAR BEHAVIOR CHARACTERISTICS OF MARINE SILTY SAND

Su Won Son, Min Jae Ko, and Jin Man Kim

Key words: direct simple shear, cyclic loading, design contour, stress ratio, undrained shear failure behavior.

ABSTRACT

Owing to the high demand for energy supply, the use of offshore wind turbines as a renewable and environment-friendly energy source has been remarkably increased. After installation in the ocean, the offshore structure foundations and soil that support them are subjected to cyclic loading from wind and waves. In this study, laboratory experiments were conducted to evaluate the shear behavior characteristics of the marine soil subjected to cyclic loading. Utilizing a cyclic direct simple shear (CDSS) test apparatus, the undrained shear failure behavior of marine silty sand was investigated. The results show that the cyclic behavior and permanent shear strain were different depending on the average shear stress ratio. Failure criteria were proposed by analyzing the failure behaviors corresponding to various cyclic loadings. The proposed failure criteria may be used for the preliminary design of offshore structure foundations.

I. INTRODUCTION

The development of environmentally friendly energy such as solar power and wind turbines, and not of thermal power and nuclear power, has been an important topic over the past few decades owing to environmental problems, such as global warming and fine dust. Wind turbines have been mostly installed on land, but their installation sites have been moving to the sea because of environmental problems such as installation space and noise. In Korea, offshore wind farms are being built around the coast of Jeju Island and the south-western coast of Korea. A structure installed in the ocean has a complex vibration transmission mechanism owing to the combined action of external dynamic loading, such as wind and waves, and internal dynamic loading, such as mechanical vibrations. The long- and short-term dynamic characteristics and resistance evaluation of offshore structures are among the significant factors in foundation design, construction, and structure maintenance.

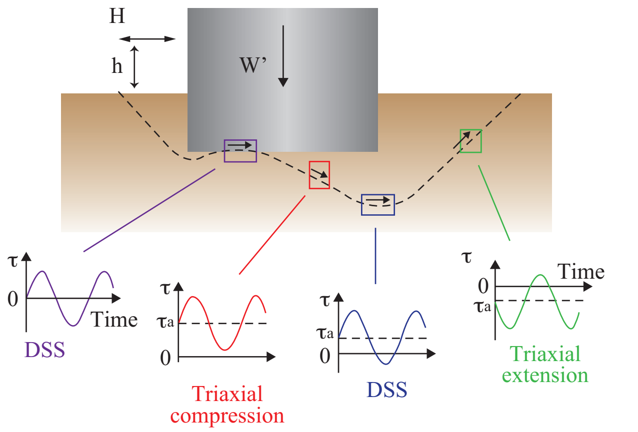

Fig. 1. Simplified stress conditions along a potential failure surface in the soil beneath a gravity structure under cyclic loading (Andersen, 2009).

Andersen and Berre (1999) investigated the behavior of soil supporting foundations subjected to cyclic loading by performing a laboratory dynamic test. It was found that the average and cyclic shear stress, drainage conditions, and stress path affect the number of cyclic loadings and failure behavior. Andersen (2009) presented a design graph with the behavior of clay, silt, and sand soils subjected to dynamic shear strength and cyclic loading. Ryu and Kim (2015) and Ko et al. (2017) presented a stress-based failure criterion for the undrained failure behavior of marine silty sand under cyclic loading with different relative density conditions. Fig. 1 shows various stress conditions when a load is applied to the structure. According to this figure, the failure surface varies depending on the location. The results from the cyclic direct simple shear (CDSS) test in this study suggest a failure surface model in which the horizontal direction dominates, as shown in the figure.

The present work is a follow-up study of Ryu and Kim (2015) and Ko et al. (2017). It evaluates the effects of the average and cyclic shear stresses on the dynamic shear behavior considering the soil relative density, and proposes 3-D failure criteria with regard to various relative densities of soil that can be used in the design procedure.

Paper submitted 05/22/17; revised 12/05/17; accepted 12/13/17. Author for correspondence: Jin Man Kim (e-mail: jmkim@pusan.ac.kr).
Department of Civil and Environment Engineering, Pusan National University, Busan, Korea.

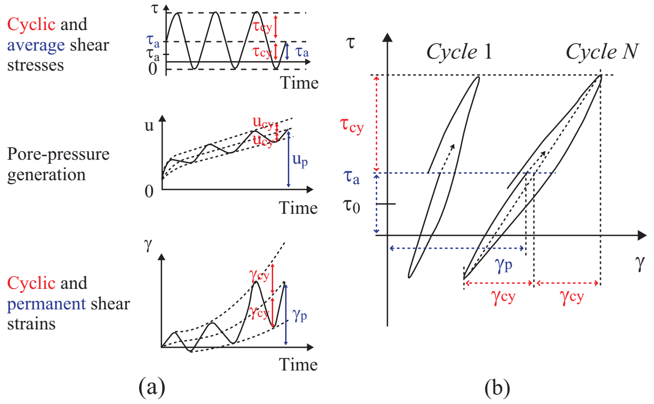

Fig. 2. Pore-pressure and shear strain as function of time under undrained cyclic loading (Andersen, 2009).

II. CYCLIC SHEAR BEHAVIOR AND FAILURE BEHAVIOR OF SOIL

1. Cyclic Shear Behavior

In general, the undrained behavior of sand depends on its relative density. In the case of loose sand, as the cyclic load acts, the sand is compressed and positive pore water pressure is generated, thereby reducing the effective stress. In contrast, in the case of dense sand, as the cyclic load acts, the sand is dilated and negative pore water pressure is generated, thereby increasing the effective stress. Therefore, loose sand shows lower shear strength, owing to positive pore water pressure, than dense sand.

2. Failure Behavior

Andersen et al. (1988) reported that the design graph expresses the cyclic stress ratio (CSR) and the average stress ratio (ASR) to the shear strain and number of cyclic loadings at the time of reaching the failure criterion. The cyclic shear stress ratio and the average stress ratio are defined by Eq. (1).

$$CSR = \frac{\tau_{cy}}{\sigma_{vc}^{`}}, \quad ASR = \frac{\tau_a}{\sigma_{vc}^{`}} \tag{1}$$

Fig. 2(a) shows a change in the cyclic and average shear stress, pore water pressure, and shear strain owing to cyclic loading. As cyclic loading is applied to the specimen under the undrained condition, pore water pressure is generated, and an increase in pore water pressure causes permanent shear strain (γ_p) and cyclic shear strain (γ_{cy}) (Andersen, 2009). Fig. 2(b) shows the behavior of the stress-strain curve caused by cyclic loading. The cyclic shear stress (τ_{cy}) generates cyclic shear strain (γ_{cy}), and the average shear stress (τ_a) generates permanent shear strain (γ_p). Accordingly, the behavior of the stress-strain relationship is different. The average and cyclic shear stresses are additional loadings, such as the stresses in the in-situ soil condition and the weight of the structure. Cyclic shear strain is the strain amplitude that occurs during one vibration, and the permanent shear strain is the strain that increases from the initial time during repeated vibration of N times.

Ishihara (1985) discovered that initial liquefaction takes place in the strain range of 2.5-3.5%, and suggested that initial liquefaction occurs in a single amplitude strain of 3%. Using laboratory experiments, Nielsen et al. (2012) defined 15% of double amplitude strain as the failure criterion. Randolph and Gourvenec (2011) proposed a strain contour using a cyclic simple shear test, and defined that the number of failures is the number of times the permanent shear strain or the double amplitude shear strain is equal to 15%, obtained from the cyclic simple shear test results with asymmetric cyclic loading on normally consolidated Drammen clay. In this study, the permanent shear strain or double amplitude shear strain of 15% was defined as the failure criterion considering the conditions of offshore structures.

The general design graph proposed by Andersen and Berre (1999) was normalized to the effective stress, while the modified design graph was normalized to the undrained shear strength considering the initial pore water pressure. After comparing the design graphs before and after implementation of the modification, it was found out that considering the vertical stress as the normalization parameter in drainage design condition is more effective than other options. However, concerning the undrained conditions, because of the importance of initial pore water pressure, the undrained shear strength is employed as the normalization parameter. In the present study, the vertical effective stress was used as the normalization parameter for cyclic and average stresses, because of the noncohesive soil under undrained condition. Hence, the values normalized with the vertical effective stress were defined as the cyclic shear stress ratio and average shear stress ratio. This is possible because of the system characteristics of the cyclic simple shear test used in this study. A description of the system characteristics is provided in Section 3.

III. CYCLIC DIRECT SIMPLE SHEAR (CDSS) TEST

1. Principle of the CDSS Test

In this study, the test was performed using a CDSS test, as shown in Fig. 3(a). The cyclic direct simple shear test reproduce the behavior of the specimen more precisely than the direct shear test, and can accurately measure the dynamic characteristics with cyclic loading during an earthquake. Soil deformation in the ground is mainly affected by horizontal seismic shear waves transmitted from the lower strata. When the ground surface is horizontal, the shear stress does not act on the horizontal plane of the ground surface before the occurrence of an earthquake. However, when an earthquake occurs, cyclic shear stress appears during vibration, in a state where the vertical stress acting on the horizontal surface remains constant. The CDSS test was performed considering a specimen under the earth pressure at rest (K_0) condition and constraining it with a wire reinforced

Table 1. Properties of west coast marine silty sand.

Min. voids ratio	Max. voids ratio	Uniformity coefficient	Coefficient of curvature	USCS	Specific gravity
0.74	1.18	1.80	0.15	SP-SM	2.62

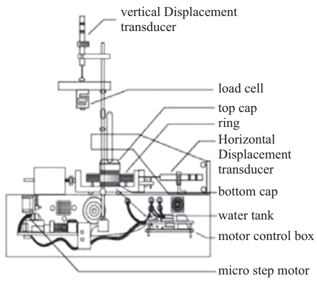

(a) Direct simple shear apparatus specification

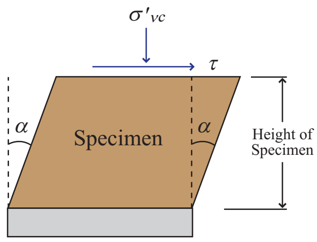

(b) Simple shear condition

Fig. 3. Simple shear condition.

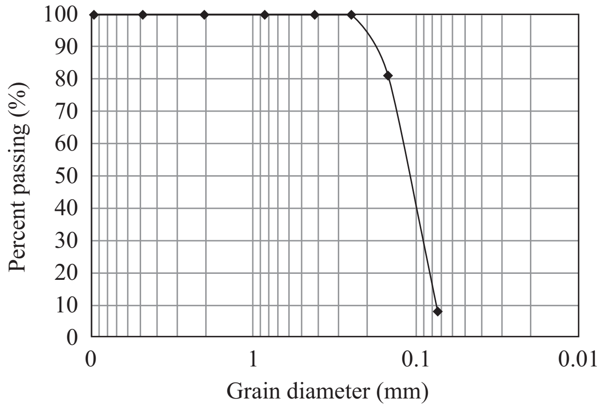

Fig.4. Grain size distribution curve (Ko et al., 2017).

membrane manufactured according to the ASTM standard D6528-07. While the shear stress is applied, the height of specimen is controlled to keep constant volume, and it is defined that the change in vertical stress is the same as the change of pore pressure under an undrained condition. Fig. 3(b) shows the principle of the direct simple shear test. The shear strain is measured when the vertical and shear stress are applied to the top part of the specimen.

2. Test Conditions and Setup

Specimens with diameter of 63.5 mm and height from 21.5 to 23.4 mm were used in the CDSS test. The initial relative density before consolidation was 50-85%. A height change in the specimen finishing consolidation was confirmed, and the relative density at this time was used. Cyclic loading with constant amplitude and period was applied to the specimen, either continuously or discontinuously. In the design of offshore wind turbine structures, it is necessary to consider the cyclic loading caused by waves and wind, and the wave loading has a period of 10 to 20 s (Andersen, 2009). In this study, the applied frequency was set at 0.1 Hz, with regard to the period of wave loading in the offshore structure. However, there is no standardized frequency for the wind, and 0.1 Hz was generally used as the frequency for the experiment. The failure criterion was applied to double amplitude shear strain and permanent shear strain of 15%. Furthermore, it was judged that liquefaction occurred at the time when the effective stress became zero, and an additional failure criterion was applied. The K_0 state was exerted by constraining the lateral displacement with a reinforced membrane, and the actual soil condition was implemented by applying the vertical consolidation stress before applying the shear stress. The vertical-consolidation stress was set at 200 kPa, within the expected stress range, on the foundation of the offshore wind turbine generator, and the CDSS test was performed after consolidating the specimen so that the height of specimen did not change during the shearing process.

This study used relatively uniform fine silty sand soils collected from the Saemangeum area near the west coast, where the construction of an offshore wind farm is planned. To analyze the soil properties, specific gravity and grain-size analyses were performed. The maximum void ratio (e_{max}) and the minimum void ratio (e_{min}) were obtained using BS1377, JSF T161-1990. Table 1 lists the soil properties of the specimens. Fig. 4 shows the grain-size distribution curve of the specimen.

Sample preparation affects the behavior of a sandy soil. The most commonly used sample preparation methods are air pluviation, water pluviation, slurry deposition, dry deposition, and moist tamping. In this study, the samples were prepared by the air pluviation method with dry tamping method. The major factors that affect the relative density of air pluviated sands are the height of particle drop (Vaid and Negussey, 1988) and rate of deposition (Miura and Toki, 1982). In the air pluviation method used in this study, the sample was dropped into the mold through the funnel and reached the membrane. Each sample was divided into five layers to obtain the same density. Saturated undrained tests can be performed on dry samples because the change in vertical stress to maintain a constant volume is the same as the change in pore water pressure under an undrained condition (Budhu and Britto, 1987). The results obtained in this way are similar to those of actual drainage shear tests (Dyvik et al., 1987). In the CDSS test, shearing is adjusted by deformation and stress control. In the strain control technique, the shear is controlled at a constant displacement rate that differs from the actual cyclic behavior. In the stress control technique, the shear is controlled at a constant stress rate, so that the actual condition is simulated. In this study, the test was performed by the stress control method because of the limitation of the test apparatus.

Table 2. Summary of the CDSS tests (Ryu, 2016).

Test ID	Relative Density, Dr (%)	Confining pressure (kPa)	Rate (/min)
CDSS_1	18.01	121.71	0.3
CDSS_2	28.78	177.21	0.3
CDSS_3	40	258	0.3
CDSS_4	52	375.64	0.3

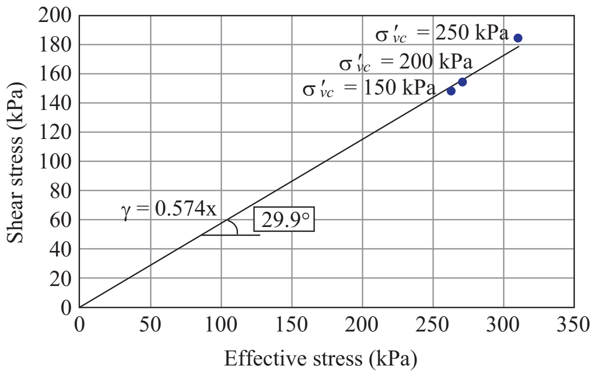

(a) Loose density

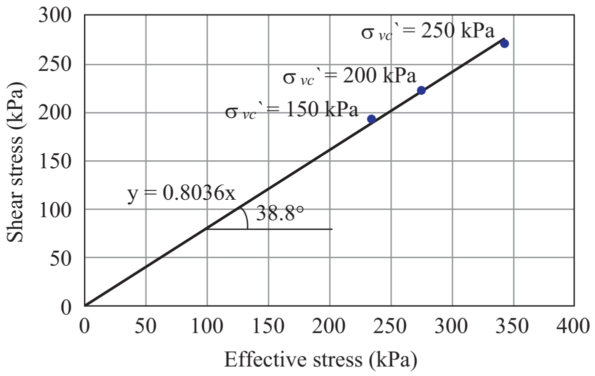

(b) Dense density

Fig. 5. Effective internal friction angle.

IV. TEST RESULTS AND ANALYSIS

Static and dynamic tests were performed under various stress conditions, and the stress behavior, shear stress, shear strain, and pore water pressure on dense and loose soil were analyzed. Finally, the 3-D stress-based failure criterion was plotted by analyzing the number of cycle loadings at failure under various stress conditions, and the equation of the stress-based failure criterion considering relative density was proposed.

1. Monotonic Test and Specimen Condition

Static tests were performed on the west coast silty sand with different confining pressures and by preparing specimens with the relative densities of loose and dense soils. Shearing was applied with a rate of 0.3 mm/min, which is similar to that of the direct simple shear test. The failure criterion was employed to

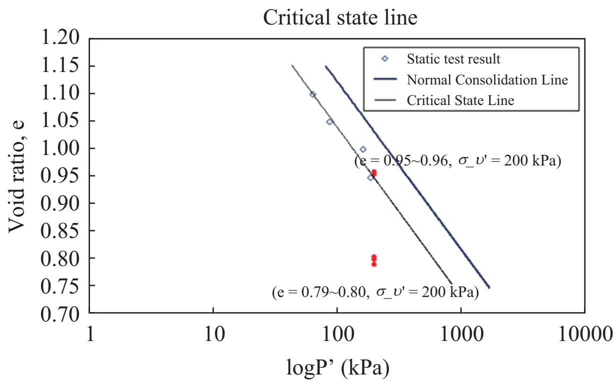

Fig. 6. Critical state line (CSL).

the shear strain of 15%, equal to that of the dynamic test in three static tests. The effective internal friction angle of each soil sample was determined using the slope angle of the fitted line from shear-normal stress curves. The obtained internal friction angles were 29.9° in loose soil and 38.8° in dense soil. The static stress ratios ($\frac{\tau}{\sigma`}$) were 0.574 and 0.804 for soil densities of 50% and 85%, respectively (Fig. 5). Note that the mentioned stress ratios were obtained when the cyclic shear stress ratio was zero, and this was considered as the initial point of the stress-based failure criterion. However, this value is approximate because the ratio of shear stress to vertical effective stress is a ratio of stresses on the horizontal plane, which is not the failure plane.

Fig. 6 shows the critical state line (CSL), which corresponds to the effective stress path of west coast sand from the results of the static test. The test was performed using the CDSS test apparatus on the effective stress-shear stress surface and connecting the points leading to failure. Table 2 summarizes the results from the static tests. The confining pressure and the relative density of each static test were obtained by a normal consolidation technique. The CSL in the undrained condition shows that the void ratio does not change and the effective stress decreases with respect to the normal consolidation line. In the P`-e space, the CSL has a shape similar to the normal consolidation line.

When analyzing the characteristics of a soil, it is generally easy to understand its compactness by using the internal friction angle, but it can be more accurately analyzed by using the CSL. In Fig. 6, the soil is divided into a loose state at the upper part of the CSL and a dense state at the lower part of it. Using the CSL, it was confirmed that the soil condition corresponding to

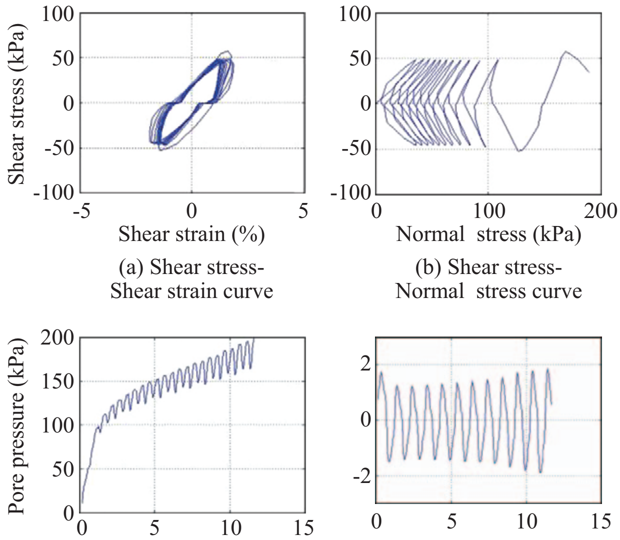

(a) Shear stress-Shear strain curve
(b) Shear stress-Normal stress curve
(c) Pore pressure as function of time under cyclic loading
(d) Shear strain as function of time under cyclic loading

Fig. 7. Stress behavior (Dr = 50%, ASR = 0, CSR = 0.3, cycles = 12).

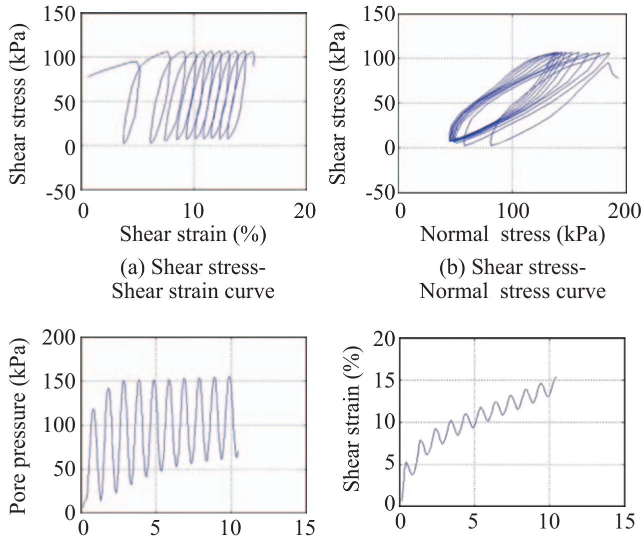

(a) Shear stress-Shear strain curve
(b) Shear stress-Normal stress curve
(c) Pore pressure as function of time under cyclic loading
(d) Shear strain as function of time under cyclic loading

Fig. 9. Stress behavior (Dr = 50%, ASR = 0.3, CSR = 0.3, cycle = 10).

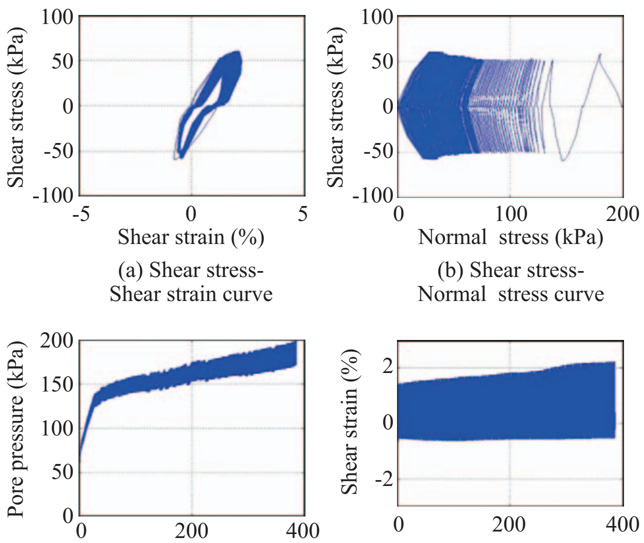

(a) Shear stress-Shear strain curve
(b) Shear stress-Normal stress curve
(c) Pore pressure as function of time under cyclic loading
(d) Shear strain as function of time under cyclic loading

Fig. 8. Stress behavior (Dr = 85%, ASR = 0, CSR = 0.3, cycles = 386).

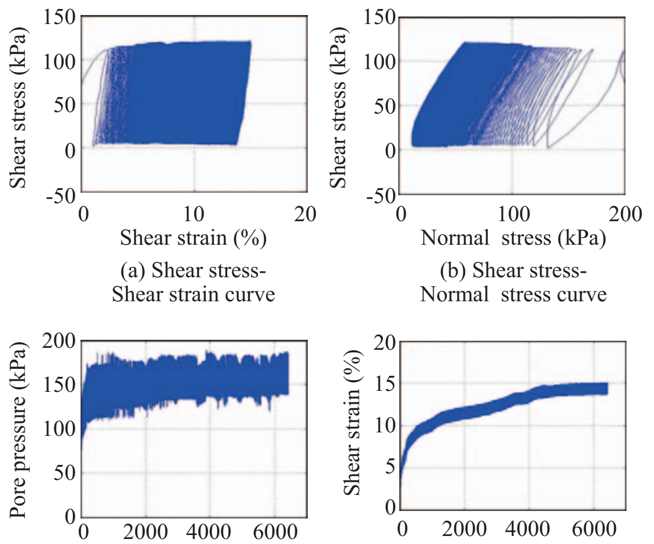

(a) Shear stress-Shear strain curve
(b) Shear stress-Normal stress curve
(c) Pore pressure as function of time under cyclic loading
(d) Shear strain as function of time under cyclic loading

Fig.10. Stress behavior (Dr = 85%, ASR = 0.3, CSR = 0.3, cycles = 6420).

85% of relative density is in the dense area; the soil condition corresponding to 50% of relative density is in the loose area.

2. Stress Behavior

CDSS tests were performed under various average shear stress ratios (0.1-0.5) and cyclic shear stress ratios (0.1-0.5).

Fig. 7 and Fig. 8 show the changes in shear stress, shear strain, and pore water pressure when the average shear stress ratio is 0 and the cyclic shear stress ratio is 0.3 at the relative densities of 50% and 85%, respectively. In these cases, the average shear stress ratio was taken as zero, on the assumption that there is no shear stress from the self-weight of the in-situ structure. In Fig. 7 and Fig. 8, when the average shear stress ratio is zero, the results of cyclic shear deformation and permanent deformation are as follows: even though the relative density was changed, the main deformation mode remained symmetrical and a slight permanent shear deformation appeared. This shows that only the shear strain increases with an increasing number of cycles. The reason is that cyclic shear strain occurs by cyclic shear stress, while permanent shear strain does not occur when the average shear stress is under zero condition. In Fig. 7 the results for the soil relative density of 50% are illustrated. The failure criterion was reached at 12 cycles, once the shear strain (permanent or average) was 15%. As can be seen, the pore water pressure increased before shear strain (permanent or average) reached the failure criterion of 15%, and failure occurred once the effective stress reached zero at 386 cycles. From the obtained results, it can be perceived that the pore water pressure in loose sand increased more rapidly than in dense sand as the cyclic loading continued. Consequently, the effective stress sharply decreased and the number of cycles at the failure state was reduced (Figs. 7(b), (d), Figs. 8(b), (d)).

Fig. 9 and Fig. 10 show changes in shear stress, shear strain, and pore water pressure when the average shear stress ratio is 0.3 and the cyclic shear stress ratio is 0.3 at the relative density of 50% and 85%, respectively. According to Fig. 9(c) and Fig. 10(c), when the average shear stress ratio is larger than 0, the permanent shear strain increases as the number of cycles increase, but the cyclic shear strain remains constant without shear strain corresponding to the applied loading. Fig. 9(a) and Fig. 10(a) show an increase in permanent shear strain under one direction, and the main deformation mode has a similar shape, even though the relative density changes.

Fig. 9 shows the results for the soil with 50% relative density under the same conditions of average shear stress ratio (0.3) and cyclic shear stress ratio (0.3). The failure criterion was reached at 10 cycles, when the shear strain (permanent or average) was 15% or more.

The failure criterion was reached at 6,420 cycles in the soil with 85% relative density, as shown in Fig. 10. This shows that although the average shear stress ratio is greater than zero, in dense sand the required number of cycles for reaching the failure criterion is far larger than in loose sand. Additionally, the pore water pressure in the dense sand drastically increases at the beginning of the cyclic loading, and then, it gradually increases as loading continues, while in the loose sand it steadily increases until the failure criterion is reached (Fig. 9(d), Fig. 10(d)).

3. 3-D Failure Criterion

The failure criterion is a combination of the cyclic shear stress ratio and average shear stress ratio reaching failure at 1-10,000 cycles. This represents five failure curves corresponding to the number of cycles. The initial point of each failure line was obtained from the static test results.

As shown in Fig. 11, when the cyclic shear stress ratio is in constant state, or when the average shear stress ratio is in constant state, the number of cyclic loadings for reaching the failure criterion decreases when the other shear stress ratio (ASR or CSR) increases. In this case, the failure curve of the loose sand has cyclic and average shear stress ratios of 0.1 to 0.2 less than those of the dense sand, and it shows a downward trend. Furthermore, failure at the dense soil mainly occurs by cyclic shear strain (double amplitude shear strain of 15%) with the average shear stress ratio close to zero. However, in the case where the average shear stress ratio increased, the failure of soil was determined by permanent shear strain rather than cyclic shear

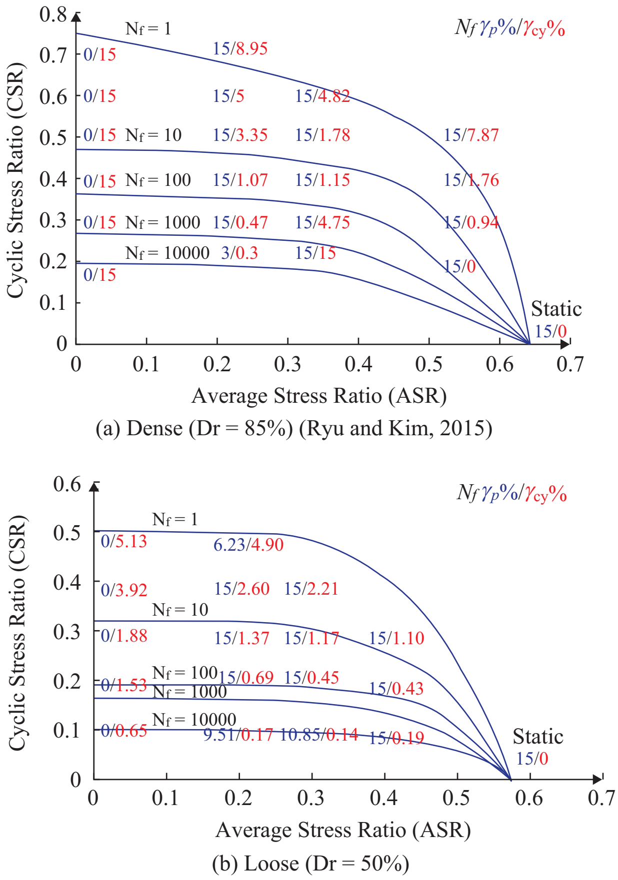

Fig. 11. Criterion lines for marine silty sand at failure (σ_{vc}` = 200 kPa) (Ko et al., 2017).

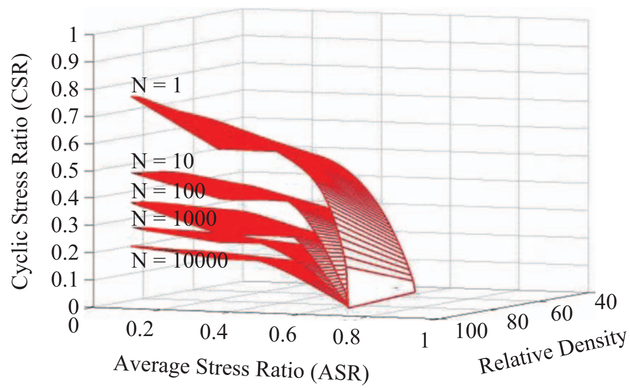

Fig. 12. Three-dimensional criterion lines for marine silty sand showing CSR, ASR, and Dr, and the corresponding cyclic and permanent shear strains at failure.

strain. Failure at the loose soil mainly occurs by the increase in pore water pressure, before the cyclic shear strain reaches 15%, with the average shear stress ratio close to zero. However, in the case where the average shear stress ratio is increased, the failure of soil was determined by permanent shear deformation rather than cyclic shear deformation.

The failure criterion for various relative densities is shown

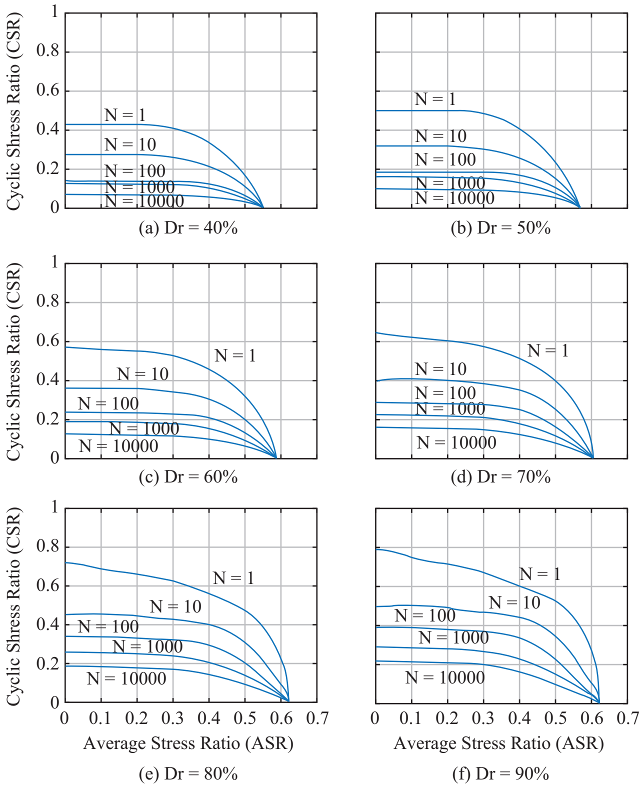

Fig. 13. Failure criterion according to relative density (σ_{vc}` = 200 kPa).

in Fig. 12 using the 3-D stress failure criterion. The 2-D and 3-D failure criterion presented in Fig. 12 and Fig. 13 can be used as a practical tool to determine the design parameters, such as cyclic shear stress ratio, average shear stress ratio, and number of cyclic loadings corresponding to the soil relative density. According to the proposed failure criterion, the failure cyclic loading is dependent on the sequence of the cyclic shear stress ratio, relative density, and average shear stress ratio.

V. SUMMARY AND CONCLUSION

To evaluate the effect of average shear stress and cyclic shear stress on the undrained shear failure behavior with regard to the relative density of silty sand, several CDSS tests were performed. The following conclusions can be drawn.

(1) Soil can be classified into loose state soil at the upper part of the CSL and dense state soil at the lower part of it.
(2) When the average shear stress ratio was zero, despite changing the relative density, the main deformation mode remained symmetrical and a slight permanent shear deformation occurred. This shows that only the shear strain increases with an increasing number of cycles. The reason is that cyclic shear strain occurs by cyclic shear stress, while permanent shear strain does not occur owing to the average shear stress.
(3) Although the average shear stress ratio is greater than zero in dense sand, the required number of cycles for reaching the failure criterion is far larger than that in loose sand. Additionally, the pore water pressure in the dense sand drastically increased at the beginning of cyclic loading, and then, it gradually increased as the loading continued, while in the loose sand it steadily increased until the failure criterion was reached.
(4) The 2-D and 3-D failure criterion given in Fig. 12 and Fig. 13 can be used as a practical tool to determine the design parameters, such as the cyclic shear stress ratio, average shear stress ratio, and number of cyclic loadings corresponding to the soil relative density.
(5) According to the proposed failure criterion, the failure cyclic loading is dependent on the sequence of cyclic shear stress ratio, relative density, and average shear stress ratio.
(6) Currently, research is being conducted to determine the failure criterion considering various confining pressures and soil relative densities.

ACKNOWLEDGEMENTS

This research was supported by the Basic Science Research Program funded by the National Research Foundation of Korea. We are grateful for their support. (NRF-2017R1A2B4010201)

REFERENCES

Andersen, K. H., A. Kleven and D. Heien (1988). Cyclic Soil Data for Design of Gravity Structures. Journal of Geotechnical Engineering 114(5), 517-539.
Andersen, K. H. and T. Berre (1999). Behaviour of a Dense Sand under Monotonic and Cyclic Loading. In Proceedings of the 12th ECSMGE, Geotechnical Engineering for Transportation Infrastructure, Amsterdam, the Netherlands, 7-10 June 1999, 2, 667-676.
Andersen, K. H. (2009). Bearing Capacity under Cyclic Loading, Offshore, Along the Coast and on Land. The 21st Bjerrum Lecture presented in Oslo, 23 November 2007. NRC Research Press Web site <www.cgj.nrc.ca>.
Budhu, M. and A. Britto (1987). Numerical Analysis of Soils in Simple Shear Devices. Soils and Foundation 27(2), 31-41.
Dyvik, R., T. Berre, S. Lacasse and B. Raadim (1987). Comparison of Truly Undrained and Constant Volume Direct Simple Shear Tests. Geotechnique 37, 3-10.
Ko, M. J., S. W. Son and J. M. Kim (2017). Relative Density and Stress-Dependent Failure Criteria of Marine Silty Sand Subject to Cyclic Loading. Journal of the Korean Geotechnical Society 33(1), 79-91.
Miura, S. and S. Toki (1982). A Sample Preparation Method and It Effect on Static and Cyclic Deformation-strength Properties of Sand. Soils and Foundation 22, 61-77.
Nielsen, S. D., A. Shajarati, K. W. Sorenson and L. B. Ibsen (2012). Behaviour of Dense Frederikshavn Sand during Cyclic Loading. DCE Technical Memorandum 15, 1-9
Randolph, M. and S. Gourvenec (2011). Taylor and Francis, London.
Ryu, T. G. (2016). Long-term dynamic behavior study of marine silty sand for offshore structure foundation design. Master's Thesis, Pusan National University
Ryu, T. G. and J. M. Kim (2015). Stress-Dependent Failure Criteria for Marine Silty Sand Subject to Cyclic Loading. Journal of the Korean Geotechnical Society 31(11), 15-23.
Vaid, Y. P. and D. Negussey (1988). Preparation of Reconstituted Sand Specimens. ASTM STP, 977. 405-417.